RESEARCH ARTICLE

Separation Modeling and Simulation of Acetone and Acetic acid Mixtures by Pervaporation Process

R. Jokar[1], M.Kazemi Moghadam*[2], M.J. Gandomi[3]

[1,2] Chemistry and Chemical Engineering, MalekAshtar University of Technology, Tehran Province, Tehran, Lavizan, Babaei Hwy, Shabanlou, QFMV+C59, Iran
[3] Hakim SabzevariUniversity, RazaviKhorasan Province, Sabzevar, Tovhid Town, 8M3J+373, Iran

ABSTRACT: The evaporation process is to separate the mixtures by partial evaporation inside the membrane. In this research, a mathematical model has been developed by considering mass and momentum transfer to model dehydration through the process of evaporation and evaporation. This process involves removing water from the liquid mixture (water / acetic acid and water / acetone) using a dense polymer membrane. The scope of the model was divided into two parts including feed and membrane. The Wilk-Chang method was used to describe the transfer of water in the feed solution, while the molecular diffusion mechanism was assumed for mass transfer within the membrane. The governing equations were numerically solved using the finite element method.Experimental data were compared and analyzed with model data. In this study, the effect of parameters such as volumetric flow rate, temperature, mass fraction as well as feed properties (flux) on the efficiency of the dehydration process was evaluated. The output was performed, the Tansig activation algorithm was used for the hidden layer, and the Purelin algorithm was used for the output layer, the results obtained by the above method were of good accuracy. Evaluation of the evaporation efficiency of the separation of acetone and acetic acid from water was compared, and finally the graphs were drawn. The error rate of these compounds at 50 ° C is 0.0191and 0.00332, respectively.Input compounds include (10% water/90% acetic acid, 10% water/ 0% acetone). We examine the flux through the membrane by Fick and Maxwell-Stephen models and compare the results with experimental data. The amount of error obtained from the comparison of experimental data and Fick model-0.0217 and -0.042, respectively, and the amount of error obtained from the comparison of experimental data with Maxwell-Stephan model, respectively-0.0144 ,-0.01.

KEYWORDS: Pervaporation, Genetic algorithm, CFD, Theory model, Fick model, Maxwell-Stephen model

https://doi.org/10.29294/IJASE.9.4.2023.3151-3163 **©2023 Mahendrapublications.com, All rights reserved**

1. INTRODUCTION

In the chemical and petrochemical industries, distillation is a well-known method for the separation of organic compounds, but due to the inefficiency of this method in the separation of azeotropes, heat-sensitive compounds, and high energy consumption, the use of new methods such as membrane processes has received much attention. In this process, the membrane is placed between two phases and the compounds in the feed are separated based on differences in molecular size, electrical charge, or their solubility in the membrane [1-2].

Among membrane processes, pervaporation is widely used due to low energy consumption, no use of intermediates for separation, and quiet operating conditions for the separation of liquid mixtures with a close boiling point, isomers, and heat-sensitive materials. The use of pervaporation to separate organic-organic and organic-aqueous compounds has gained special importance in recent years [3]. In pervaporation, the feed compounds in the liquid phase are in contact with the upstream of the membrane, and by applying a vacuum driving force; the product is separated and evaporated as a vapor downstream of the membrane-based on differences in adsorption rate and

**Corresponding Author:mzkazemi@gmail.com*
Received: 28.04.2023 **Accepted:** 17.05.2023 **Published on**: 22.05.2023

penetration into the membrane. Usually, a vacuum pump or carrier gas is used to create a vacuum on the product side. The product, which is in the form of steam, is converted into a liquid form by a refrigerant and collected. In this process, the amount of mass transfer through the membrane depends on factors such as downstream pressure, temperature, and thickness of the membrane. When the downstream pressure of the membrane is very low, the amount of product is inversely related to the thickness of the membrane. Mass transfer through a thick film is a very slow process and prevents the use of pervaporation in breaking azeotropes [4]. Figure (1) shows a schematic of this process.

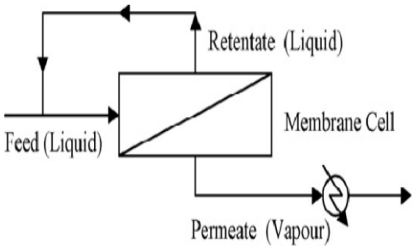

Figure 1: Schematic of pervaporation membrane process

The process of pervaporation was first introduced by Kuber in 1917. He reported rapid evaporation of water from aqueous solutions through bags of cellulose nitrate. In 1935, Farber made the first attempts to concentrate the protein solution using evaporative leaching. In 1965, Heisler et al.,[5] conducted the first quantitative study of pervaporation to separate aqueous ethanol mixtures using cellulose membranes. Due to the attention of the petrochemical industry to the separation of hydrocarbon mixtures, Bening et al., at 1958 used ethyl cellulose and polyethylene membranes to separate the normal mixture of heptane and isooctane and a polyvinyl alcohol membrane for dehydration. Binning et al.,[6] established the principles of pervaporation and pointed to the commercial potential of pervaporation for the separation of azeotropes and other organic mixtures. In 1980, the first commercial membrane developed by GFT, now owned by Solzer, was introduced and used to dehydrate ethanol. This membrane had a composite structure consisting of a dense selective layer of polyvinyl alcohol. The first pilot plant was launched by GFT in Brazil. In 1980, the Membrane Research and Technology Company (MTR) developed the first composite membrane to separate volatile organic compounds (VOCs) from water. After that, many evaporative leachate factories were established in the world. For example, from 1984 to 1996, 38 solvent dehydration plants were set up for ethanol and iso-propanol, eight units for other solvents such as esters, and one unit for the recovery and recycling of volatile organic compounds [7]. Evaporative leakage process modeling was first performed in 2011 by Hu Hyu et al., for concentrated hydrogen peroxide [8]. Mashallah Reza Kazemi et al.,[9] applied the CFD code to model the removal of water from the water/ethylene glycol mixture by the pervaporation process in 2011. In 2014, Mostafa Keshavarz Moroji et al.applied a CFD code to model the removal of water from the water/ethanol mixture by the evaporation process [10]. Evaporation of the evaporation process was first modeled by using MATLAB genetic algorithm in 2004 by Kittisupakorn-Pasian and coworkers, to control the membrane reactor [11]. In 2013, Yaser Shirazi et al., examined the modeling of a genetic algorithm to investigate the operating conditions on the performance of pervaporation with PVA membranes [12]. Mansour Kazemi Moghaddam performed modeling of dehydration of organic compounds using polymer membranes using a neural network in 2017 [13].

In this research, a mathematical model has been created by considering mass and momentum transfer to model dehydration through the pervaporation process. This process involves removing water from a liquid mixture (water / acetic acid, and water/acetone) using a dense polymer membrane. The scope of the model was divided into two parts including feed and membrane. The Wilk-Chang method is used to describe the transfer of water in the feed solution, while the molecular diffusion mechanism is assumed to transfer the mass into the membrane. The governing equations are solved numerically using the finite element method. Experimental data will be compared and analyzed with model data. In this study, the effect of parameters such as volumetric flow rate, temperature, mass fraction as well as food properties (flux) on the efficiency of the dehydration process was evaluated. The output was executed. The Tansig activation algorithm was used for the hidden layer and the Purelin algorithm was used for the output layer.

2- MODELING AND SIMULATION

Mathematical modeling is the basis of simulation of advanced processes and units on an industrial scale and is of particular importance. The first step is relational modeling, which can use three methods: mass, differential and integral. The second step is to solve the equations obtained from modeling, which according to this study is done by numerical solution method because due to the existence of complex geometries and also the simultaneous occurrence of various phenomena (momentum transfer, heat and mass transfer, chemical reactions, etc.) Equations obtained by analytical methods are impossible. In non-ideal modeling processes, the model usually leads to the production of multiple and nonlinear equations that are not possible to solve the equations analytically and simultaneously, and despite the simplistic assumptions in the applied model, the need to use numerical and computer methods to solve equations. The model is quite impressive [14]. One of the numerical methods that are used successfully in various fields of engineering is the finite element method (FEM) [15].

Computational fluid dynamics is a very powerful modeling tool that uses fast computers and applied mathematics to model fluid flow to predict heat and mass transfer heat transfer and to optimally design industrial processes. The measure of success is the degree of agreement between the results of numerical modeling and laboratory results in samples that can be accurately performed [16].

2-1- Governing equations

An acceptable degree of separation of an evaporative seepage membrane for a two-component mixture is called the separation coefficient (α), which can be calculated by Equation (1):

$$\alpha = \frac{X_{p,i}/X_{p,j}}{X_{f,i}/X_{f,j}} - - - -(1)$$

Where $X_{p,i}$ and $X_{p,j}$ are the molar fractions of the permeable components (on the product side) and $X_{f,i}$ and $X_{f,j}$ are the same molar fractions in the feed, respectively. The separation coefficient can vary from one to infinity, and larger αs indicate greater selectivity. Since the separation coefficient is measured experimentally, it expresses a combination of the overall performance of the system and, depending on the hydrodynamic conditions of the feed, product side resistance due to high partial pressures, changes in diffusion rate due to membrane swelling or changes in component membrane solubility. To change, the separation coefficient as a function of the seepage flux term can also be defined as Equation (2) [17]:

$$\alpha = \frac{X_{f,j}J_i}{X_{f,i}J_j} - - - -(2)$$

J_i and J_j are component fluxes. Similarly, J_k is the total seepage flux for the k component (which is k = i or k = j for the two-component feed) in the form of relation (3) [18]:

$$J_k = \frac{C_{f,k} - C_{p,k}H_k}{R_{ov,k}} \quad (3)$$

$C_{p,k}$ and $C_{f,k}$ are the concentrations of feed and product, and H_k is the relative dimensionless equilibrium coefficient ($C_k^{vap}/C_k^{liq} = H_k$) and $R_{ov,k}$ is the total mass transfer resistance. Under certain conditions of evaporative seepage, the total pressure of the second side is much less than the vapor pressures of the seepage component, and the assumption $C_{p,k} \sim 0$ is acceptable. It should be noted that in many cases, $C_{f,k} >> H_k$ is $C_{p,k}$, so the separation coefficient can be written by combining equations, in terms of component resistance as relation (4) [19]:

$$\alpha = \frac{R_{ov,j}}{R_{ov,i}} - - - -(4)$$

Overall component resistance ($R_{ov,k}$) as shown in Equation (5), the sum of the mass transfer resistors on the feed side ($R_{f,k}$), the membrane ($R_{m,k}$) and the product side ($R_{p,k}$) is [20]:

$$R_{ov,k} = R_{f,k} + R_{m,k} + R_{p,k} - - - -(5)$$

If the pressure on the product side is very low, $R_{p,k}$ can be ignored compared to the other two resistors.

The mass survival equation can be used to describe the transfer of water from the feed phase to the side of the leaked component. The differential form of the survival equation for water is Equation (6):

$$\frac{\partial C_W}{\partial t} + u\nabla C_W = \nabla(-D_W \nabla C_W) + R_W - - - (6)$$

In this relation C_w water concentration, D_w diffusion coefficient, u velocity vector and R_w water reaction velocity which in this case is equal to zero.
In addition, the motion equation (Navier-Stokes equation) to obtain the feed velocity distribution on the membrane module side is in relation (7):

$$\rho \frac{D_u}{D_t} = -\nabla P + \mu \nabla \hat{} 2u + \rho g \text{ ---------- (7)}$$

The equations of momentum conservation and mass conservation must be summed and solved simultaneously.
The mass transfer equation for water transfer in the feed phase can be simplified as shown in Equation (8).

$$D_{w,f}\left[\frac{\partial^2 C_{w,f}}{\partial x^2} + \frac{\partial^2 C_{w,f}}{\partial y^2}\right] = u_y \frac{\partial C_{w,f}}{\partial y} \text{ ---------- (8)}$$

The boundary conditions of the continuity equation on the feed side are:

$$y=0, C_{w,f}=C_0 \quad \text{(Input concentration) ---(9)}$$
$$y=l, \frac{\partial C_{w,f}}{\partial y} = 0 \quad \text{(Insulation) ---------- (10)}$$
$$x=0 C_{w,f} = 0 \text{(convection flux) ----------(11)}$$
$$x=x_1, \; C_{w,f} = \frac{C_{w,m}}{m} \text{(convection flux) --------(12)}$$

The condition of the convective flux boundary assumes that all the masses passing through this boundary are convective. It is assumed that any mass flux due to infiltration at this boundary is zero. Which in the above equation (m) is the partition coefficient for water between the feed and the membrane.
In steady state and slow flow, Equation (7) is simplified as follows:

$$-\nabla P + \mu \nabla^2 u + \rho g = 0 \text{ ----------(13)}$$

The boundary conditions for the Navier-Stokes equation on the feed side are [21]:

$$X=0, \quad P=p_m \text{ ----------(14)}$$
$$X=x_1, \; u_y=0 \text{ ----------(15)}$$
$$y=0, \quad u_y=u_0 \text{ ----------(16)}$$
$$y=l, \quad u_y=0 \text{ ----------(17)}$$

Water diffusion coefficient in acetone and acetic acid are calculated by the Wilk-Chang equation. This equation is used to penetrate a very dilute environment as Equation (18).

$$D_{ij}^0 = \frac{7.4 * 10^{-8} (\emptyset M_i)^{.5} T}{\mu_i \vartheta_j^{.6}} - - - - - - - - - (18)$$

Where D_{ij}^0 is the water diffusion coefficient in acetone and acetic acid (cm^2/s), M_i is the molecular weight of water, T is temperature (K), μ_i is water viscosity (cP), ϑ_i is the molar volume of acetone and aceticacid (mol/cm^3) And $\emptyset$ water accumulation factor, which forms the hydrogen bond.

The diffusion coefficient was then modified with Vignes. This equation is to consider the effect of concentration. Vignes suggested that the ratio of components depends on the penetration of a binary mixture ij expressed by Equation (19):

$$D_{ij} = (D_{ij}^0)^{x_j} (D_{ji}^0)^{x_i} - - - - - (19)$$

The density of the solution is determined by Equation (20):

$$\rho_m = \Sigma \rho_i x_i - - - - - (20)$$

ρ_m is the density of the solution (kg / m3), ρ_i is the density of each component (kg/m3), and x is the weight fraction of each component. The membrane continuity equation is written as Equation (21):

$$D_{w,m}[\frac{\partial^2 C_{w,m}}{\partial x^2}+\frac{\partial^2 C_{w,m}}{\partial y^2}]=0-(21)$$

The boundary conditions for steady state equation in the membrane are:

$X=x_1, C_{w,m}=C_{w,f}*m$ -----(22)

$X=x_2 C_{w,m}=0$ ----------(23)

$y=0 \quad \frac{\partial C_{w,m}}{\partial y}=0$ ---(24)

$y=l \frac{\partial C_{w,m}}{\partial y}=0$ ----------(25)

2-2- Model assumptions

The assumptions of water concentration distribution are:

- Temperature and pressure are constant during the process.
- The flow is considered slow.
- The system is solved independently of time.
- Heat transfer phenomenon is ignored.
- There is no production and consumption of crime.
- No chemical reaction occurs.

Membrane penetration is one-dimensional and the size, distribution and diameter of the pores are uniform [22].

2-3- Model geometry

The geometric shape of the membrane in two-dimensional space is defined as a rectangle of length y and width x according to Figure (2).

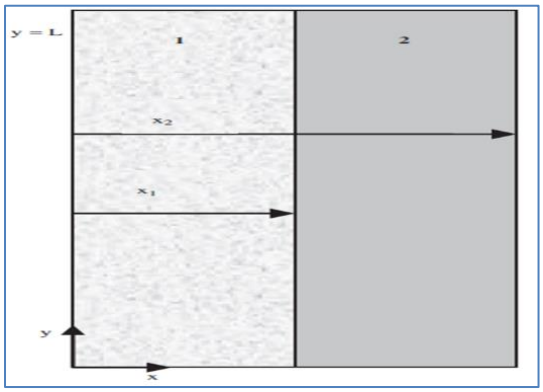

Figure 2 - Model areas and related boundaries

2-4- Simulation

This model is for the stable transfer of organic compound through the membrane. The mixture of acetone / water and acetic acid / water enters (y = 0, feed side) and exits (y = L). Water diffuses through the membrane due to the concentration gradient (x direction). In this process, the liquid mixture is placed on one side of the membrane and the component leaks faster than the other components to the other side of the membrane. The seepage component on that side collects as steam downstream. Using the designed CFD code, the momentum equation and mass transfer are solved simultaneously for the evaporation process.

2-4-1- Modeling using CFD

Using the designed CFD code, the evaporation process was performed for a mixture of water / acetic acid and water / acetone.

2-4-1-1-Water / acetic acid mixture

The parameters used for the mixture of water and acetic acid are given in Table (1).

The velocity distribution and velocity profile on the feed side can be seen in Figure (3). According to Figure (3A), the velocity in the middle of the tube has its maximum value and as it moves towards the side of the tube, the velocity of the fluid decreases until the velocity reaches zero in the membrane wall and as the fluid moves forward, the velocity of the fluid decreases. The membrane penetration phenomenon occurs and some of the fluid is purified and exits in the X direction.

Figure (4A) shows the distribution of water concentration on the feed side. Concentration changes near the membrane wall are large and in areas far from the membrane the concentration changes are negligible equal to the feed concentration. Due to the high velocity and short membrane length, the concentration polarization in the system is very low. Figure (4B) shows that the water concentration in a large amount of feed is almost constant while a sharp decrease in water concentration is observed in the vicinity of the membrane wall.

Due to the fact that penetration into the membrane occurs slowly, there is no velocity distribution on the membrane side, the distribution of water concentration on the membrane side is shown in Figure (5A) and the water concentration profile on the membrane side is shown in Figure (5B). Since the vacuum condition is assumed that only water penetrates through the membrane, the concentration profile in the X direction is linear and uniform. The top and bottom sides of the membrane (y = 0, y = l) are assumed to be insulated. The concentration of water at the interface between the feed and the membrane is always the highest, and as we move in the X direction, the concentration of water decreases sharply, reaching zero at the membrane boundary.

Table 1- Parameters used in modeling water / acetic acid mixture

value	Parameter	value	Parameter
$1.33 * 10^{-10}$	Wilk-Chang diffusion (m^2/s)	1	Food pressure (atm)
0.4	Partition coefficient	0.0002	Feed channel size (m)
$3.7 * 10^{-12}$	Water penetration through membrane layers (m^2/s)	0.0004	Effective module length (m)
0.1	Mass fraction of water at the inlet	0.0001	Membrane layer thickness (m)
0.00026	Feed speed at module input (m/s)	303	Feed temperature (K)

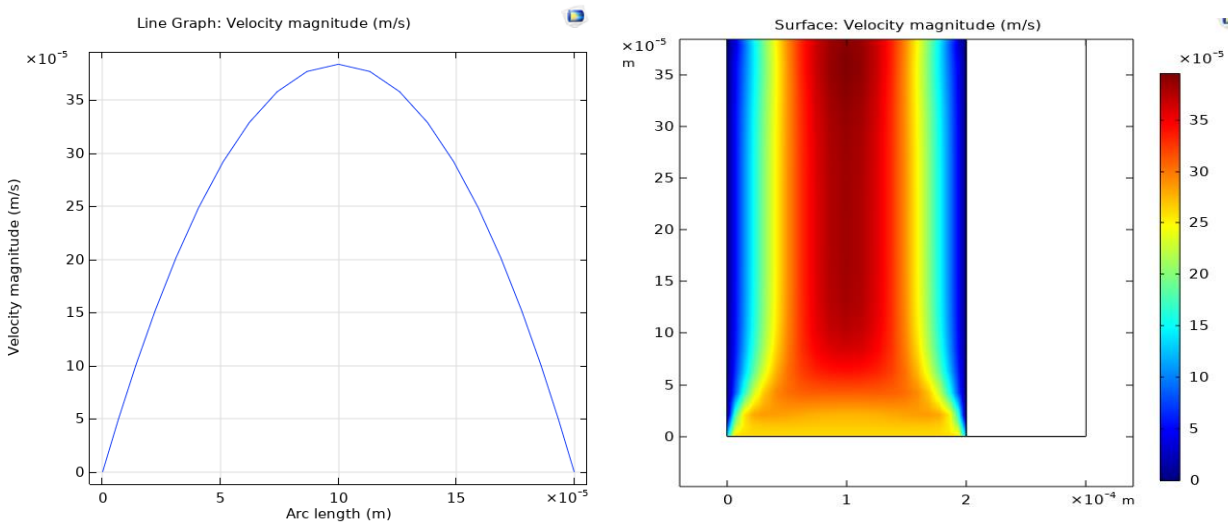

Figure 3- A: Velocity distribution B: Velocity profile on the feed side for water (water / acetic acid mixture)

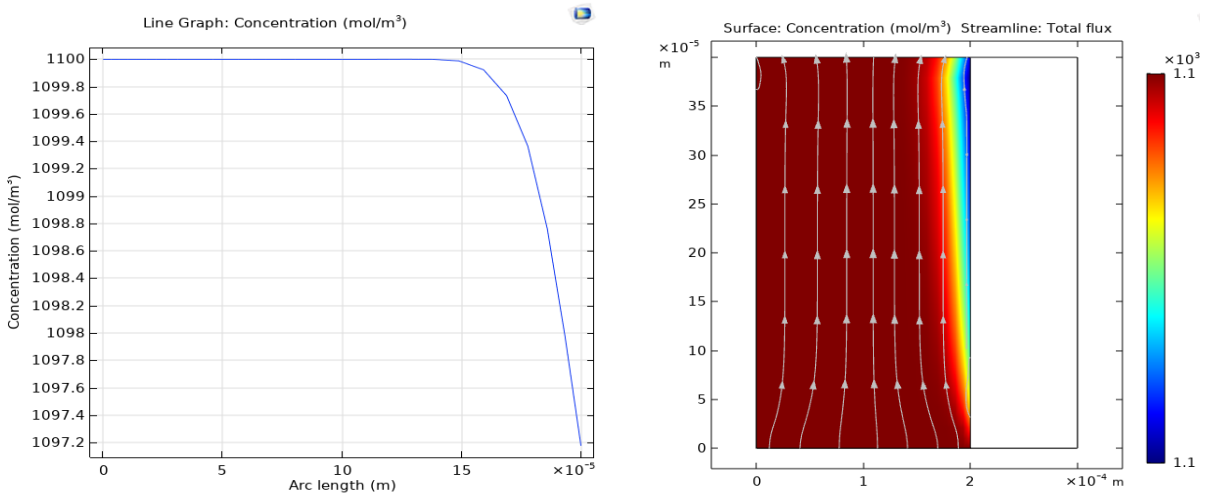

Figure 4- A: Concentration distribution B: Concentration profile on the feed side for water (water / acetic acid mixture)

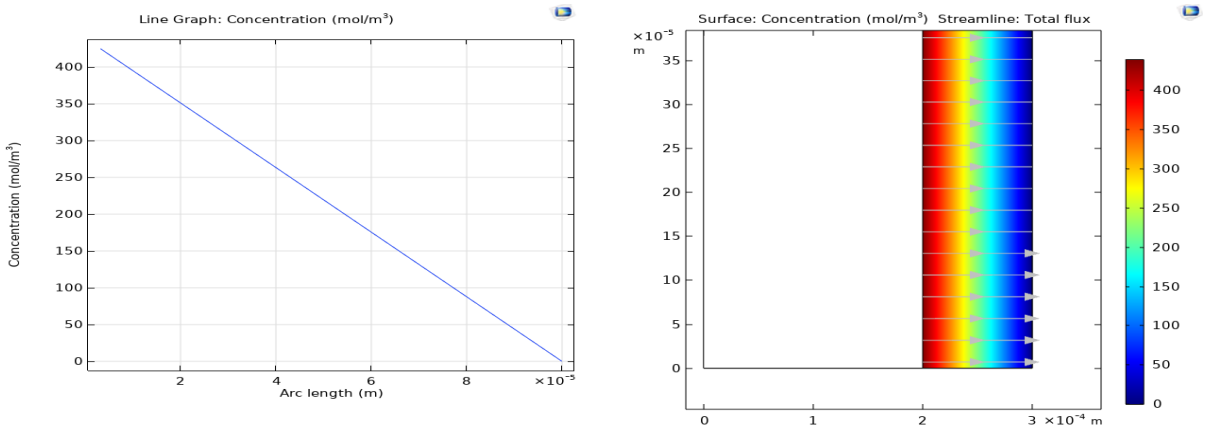

Figure 5- A: Concentration distribution B: Concentration profile in membrane for water (water / acetic acid mixture)

2-4-1-2- Water / Acetone Mixture

The parameters used for the water-acetone mixture are given in Table (2).

Table 2 - Parameters used in modeling water / acetone mixture

value	Parameter	value	Parameter
$2/30 * 10^{-9}$	Wilk-Chang diffusion (m^2/s)	1	Food pressure (atm)
0.4	Partition coefficient	0.0002	Feed channel size (m)
$4/20 * 10^{-11}$	Water penetration through membrane layers (m^2/s)	0.0004	Effective module length (m)
0.1	Mass fraction of water at the inlet	0.0001	Membrane layer thickness (m)
0.003	Feed speed at module input (m/s)	323	Feed temperature (K)

Similar to the previous cases, as shown in Figure 6, the velocity in the middle of the tube has its maximum value, and as it moves to the side of the tube, the velocity of the fluid decreases until the velocity reaches zero in the membrane wall, and as the fluid moves forward, The velocity of the fluid decreases.

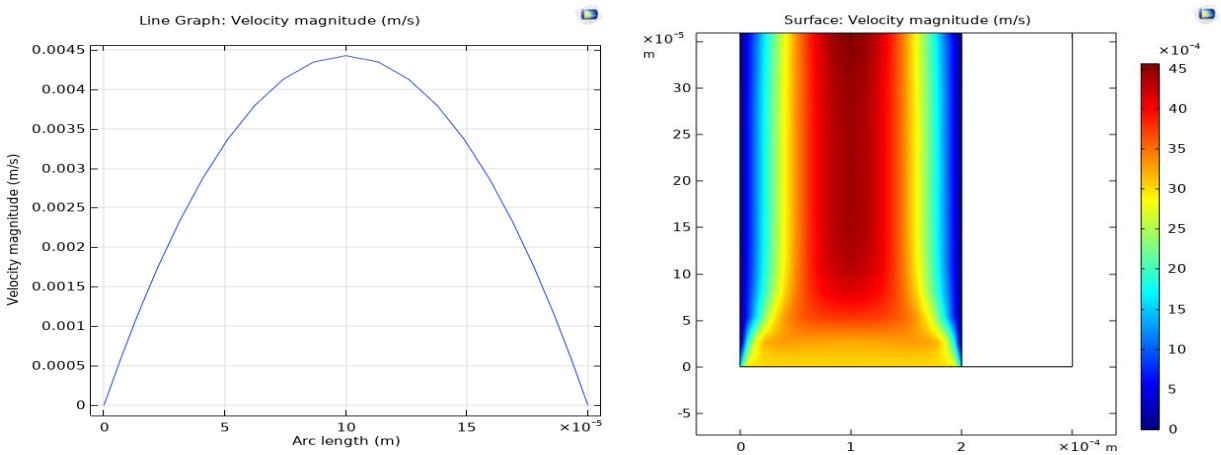

Figure 6- A: Velocity distribution B: Velocity profile in feed for water (water / acetone mixture)

Figures (7A) and (7B) show the distribution of water concentration in the feed for the water / acetone mixture, respectively.

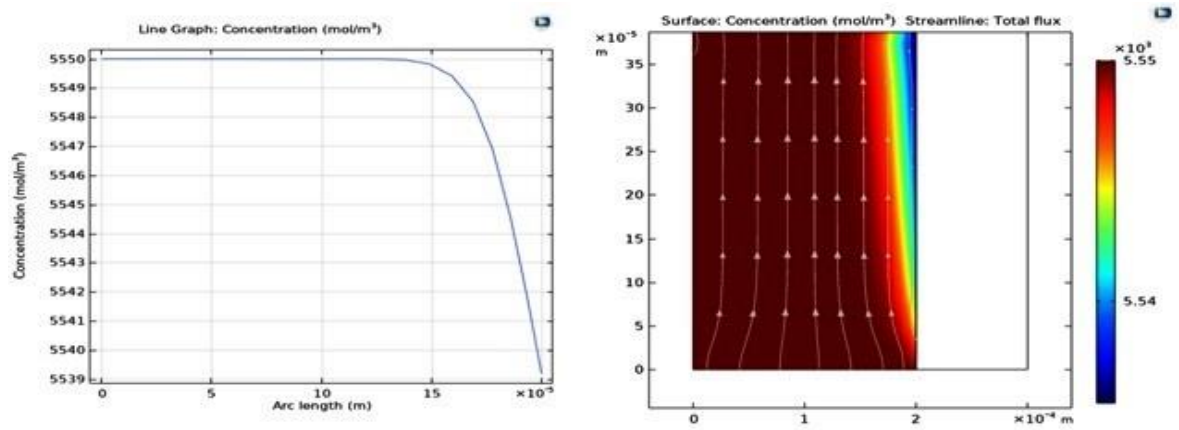

Figure 7- A: Concentration distribution B: Concentration profile in feed for water (water / acetone mixture)

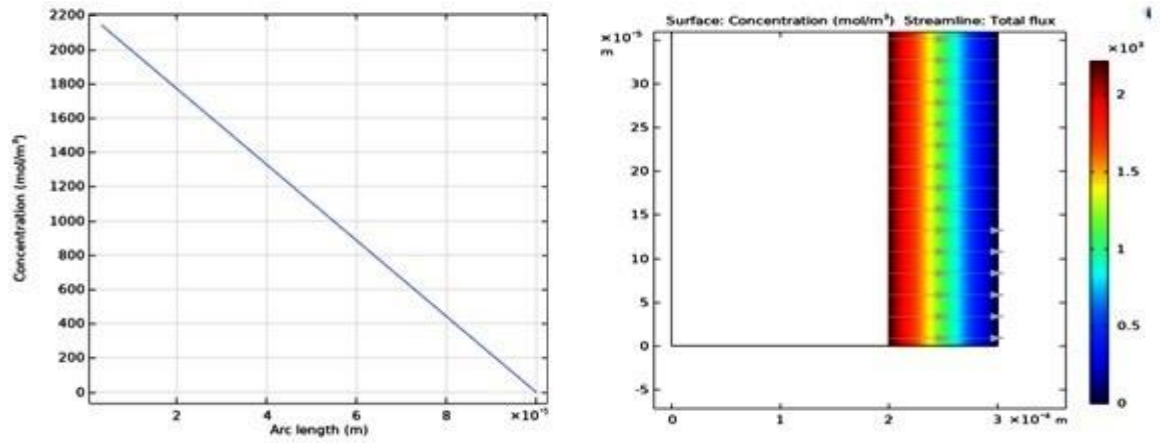

Figure 8- A: Concentration distribution B: Concentration profile in membrane for water (water / acetone mixture)

The distribution of water concentration in the membrane is shown in Figure (8A) and the water concentration profile in the membrane is shown in Figure (8B). Since the vacuum condition is assumed that only water penetrates through the membrane, the concentration profile in the X direction is linear and uniform. The concentration of water at the interface between the feed and the membrane is always the highest, and as we move in the X direction, the concentration of water decreases sharply, reaching zero at the boundary of the membrane.

2-4-2-Modeling of dehydration of organic compounds using neural network

In this study, Levenberg-Marquardt multilayer perceptron and functional ANN with 3 inputs and one output were used. The Tansig transfer function is used for the hidden layer, the Purelin for the output layer. 10 neurons were used for the hidden layer. After processing the data, 70% is allocated for learning, 15% for validation, and the remaining 15% for testing. Figure (9) shows a schematic of a two-layer ANN schematic for water / acetone mixture with only one hidden layer and an outlet. The inputs are multiplied by a value of, and there is a bias factor (b) that is added to the input (the bias is a constant value that is added to the input to increase accuracy). The result is then subjected to a function and the resulting value is multiplied by a weight and added by a bias. The end result transfers another function (with a different shape and function) and an output is generated. There are 10 nerve cells and 3 inputs in the first layer. However, the number of neurons in the output layer is the same as the number of outputs.

The whole method is displayed through some of the status bars in the progress box. The initial values are displayed on the left side of the status bar and the current value is displayed on the right.

Epoch is accepted from 0 to 1000 iterations. This means that the weights are changed

consecutively for 1000 times based on the Levenberg-Marquardt function and the training method is performed. If the number of repetitions reaches 1000, the method stops.

There was no time limit (but it can be set to a period that stops after, say, 30 seconds). Yield initially was 0.211 for water / acetone and 0.00183 for water / acetic acid. If this value reaches 0, the error is acceptable. Gradient is an error function and means the amount of derivatives. The range of this variable for water / acetone starts from 0.51 and water / acetic acid from 0.00431. Validation check is the maximum number of times a network failure can be tolerated.

As shown in Figure (10), the network performance for Train, Validation and Test has been reduced to an acceptable level. The phases marked with a circle in the figure are the best validation performance for water / acetone 3 and water / acetic acid 17.

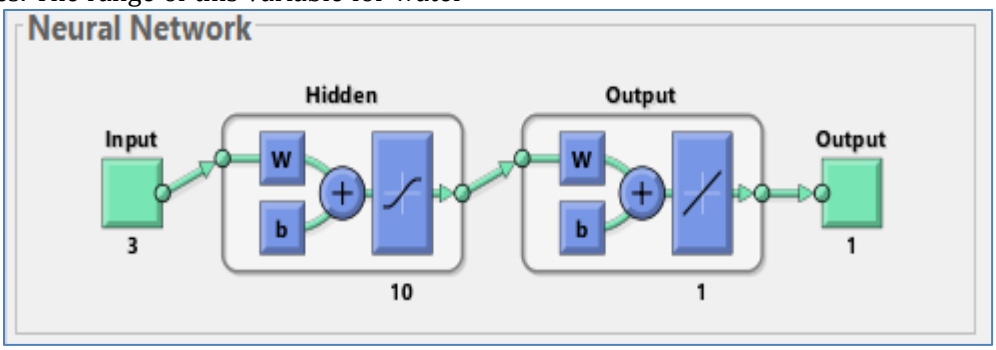

Figure 9 - Schematic view of ANN network of water / acetone mixture

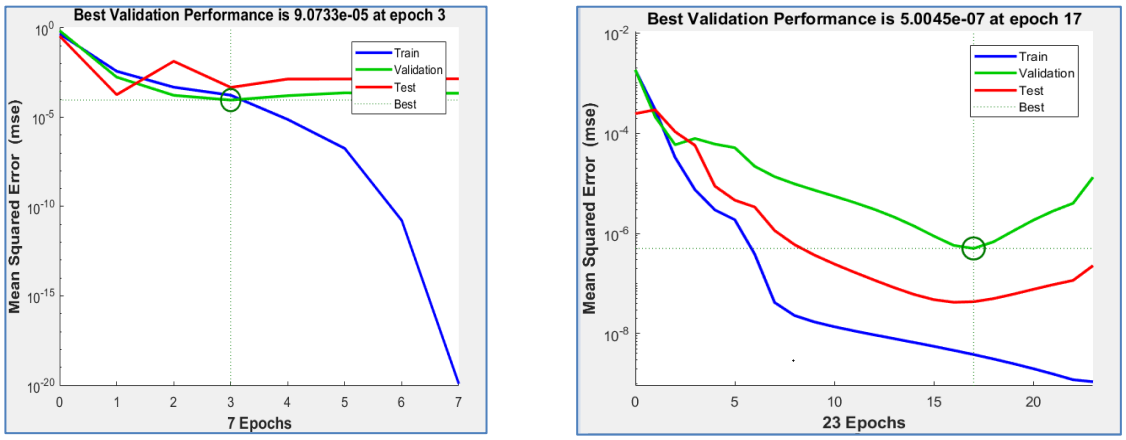

Water / Acetone **Water / Acetic acid**

Figure 10- Dehydration performance diagrams

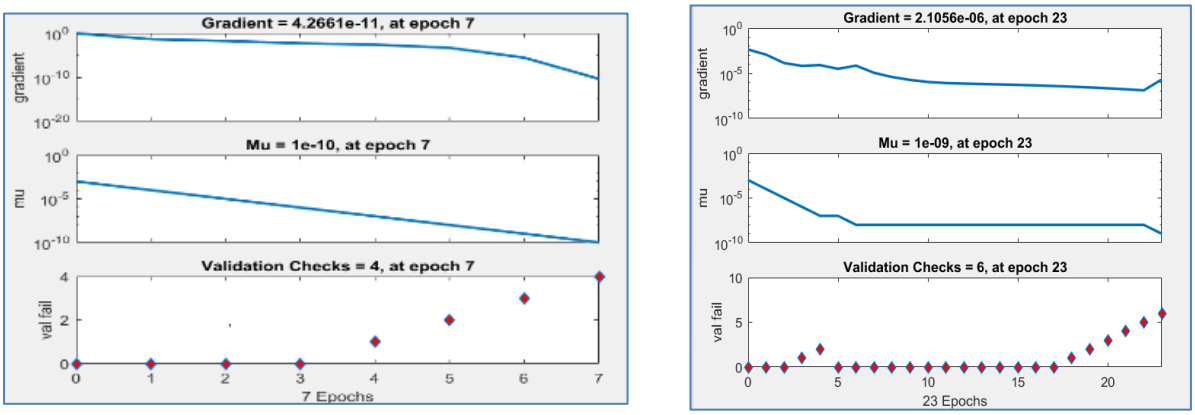

Water / Acetone **Water / Acetic acid**

Figure 11- Dehydration training diagram

Figure (11) shows the training situation diagram showing the different situation in the training stage for each of the mixtures. The first diagram is related to the slope error function. The second is for Mu, and the third is for invalidation. Figure (12) shows the regression diagram. The horizontal output axis shows the target parameters, displays the vertical axis of the ANN output. If ANN can model accurately, the graph must be a line ? = ((a line with a slope of 1 that passes through the origin of the coordinates). To statistically calculate the best line with the least error, the linear equation obtained in the whole diagram should be used:

Water / Acetone $Output=1\times Target+0.0064$

Water / Acetic acid $Ouput=1\times Target+0.0043$

If the value of F is closer to 1, it means that there is a small difference between the target outputs and the ANN outputs in the modeling. In general, the regression coefficient for all water / acetone data is 0.99691 and water / acetic acid is 0.999985 and which is a very good result.

As shown in Figures (13) and (14), for all four mixtures, by comparing the neural network performance with the experimental results, the neural network model was able to predict the experimental data well and the resulting error is less than 1%.

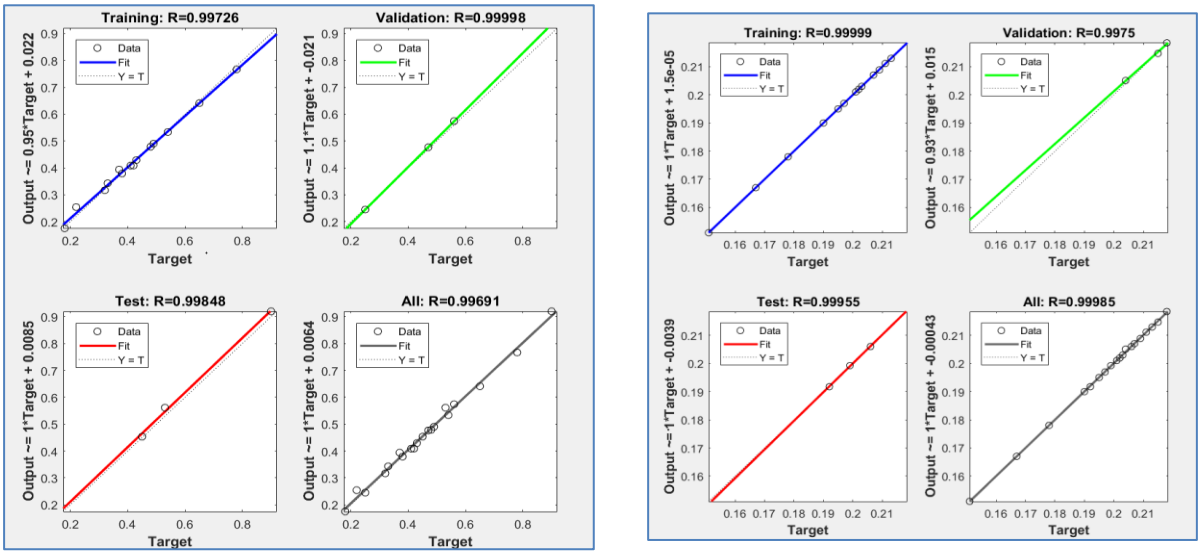

Water / Acetone **Water / Acetic acid**

Figure 12- Dehydration regression diagram

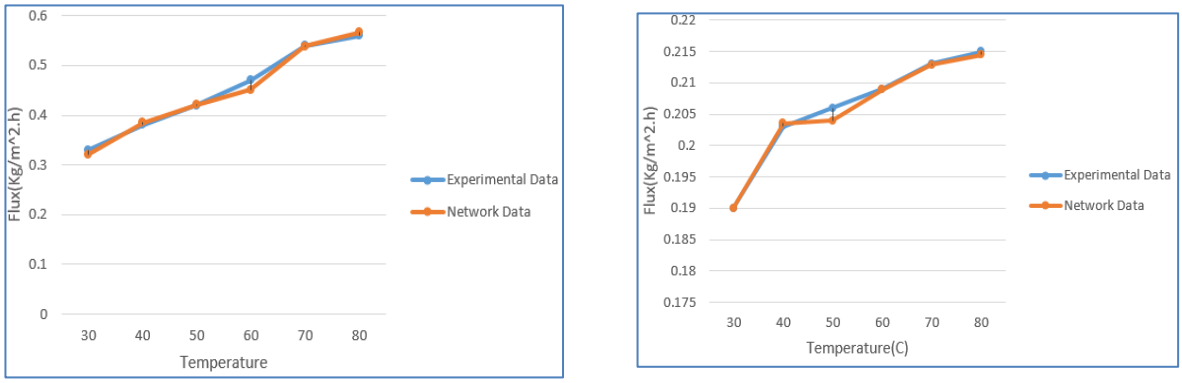

Water / Acetone **Water / Acetic acid**

Figure 13 - Comparison of ANN model data and experimental data (flux-to-temperature parameter)

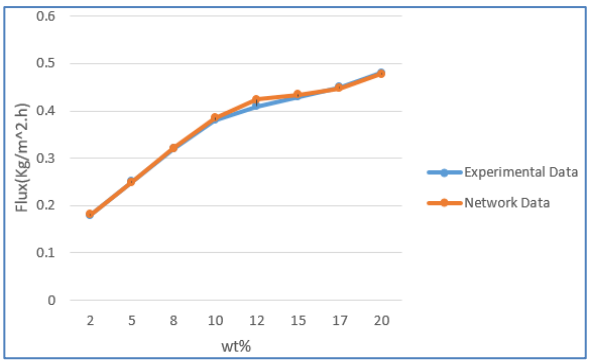

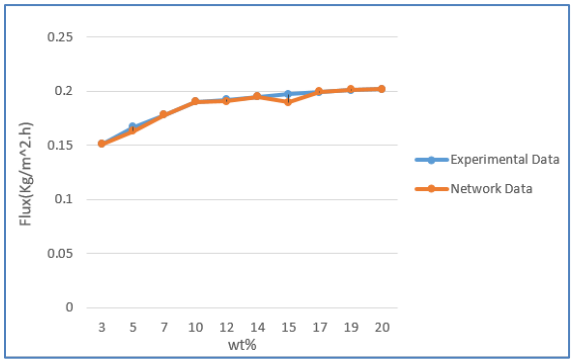

Water / Acetone **Water / Acetic acid**

Figure 14 - Comparison of ANN model data and experimental data (flow parameter to mass fraction)

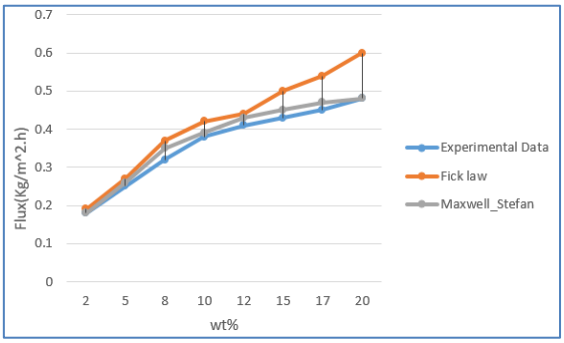

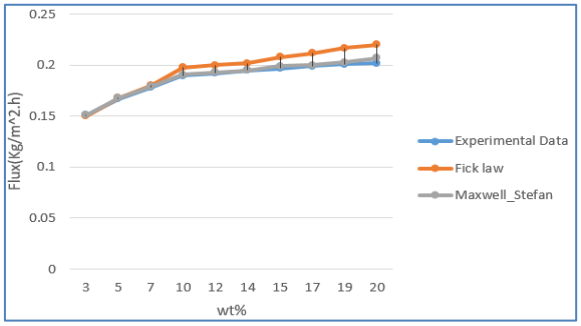

Water / Acetone **Water / Acetic acid**

Figure 15- Graph of flux changes in mass fraction

The flow rate across the membrane relative to the mass fraction was calculated using models and compared with laboratory data. With this comparison, the best model was selected to provide a theoretical relationship to obtain the flux. Figure (15) plots flux-to-mass fraction diagrams for laboratory data, Fick's law, and Maxwell-Stephen theory were plotted and compared.

As shown in Figure (15), a diagram of the flux changes with respect to the mass fraction was drawn. By comparing the laboratory data with the data obtained from the models, it is determined that the Maxwell-Stephen model with the data Laboratory compliant and can predict membrane flux with less error than laboratory data. As you can see in Table (3), by comparing the experimental data with the data obtained from the genetic algorithm model, we obtain the error rate. Input compounds include (10% water / 90% acetic acid and 10% water / 90% acetone). By comparing these mixtures at different temperatures, we see that these errors are very low.

Table 3 - Error rate of genetic algorithm with experimental data

Temperature	Water / acetic acid mixture	Water / acetone mixture
50	-0.0098	-0.00323
60	-0.000478	-0.0199
70	-0.000496	-0.00185
Total error	0.0107	0.025

As you can see in Table (4), by comparing the experimental data with the data obtained from the theoretical models, we obtain the error rate. By comparing these mixtures in the combination of different percentages in the input feed, we see that the amount of error obtained in the Maxwell-Stephen model is less than the amount of error obtained in the Fick rule model. Comparing the experimental data with the Fick theory model, we see that the

water / acetone mixture has the highest error rate. Comparing the experimental data with the Fick theory model, we see that the water / acetone mixture has the highest error rate.

Table 4- Error rate of theoretical models with experimental data

Weight percent of organic compound	5	10	15	20	Total error
Water / acetic acid mixture (Fick Law)	-0.079	-0.0217	-0.041	-0.1	0.2417
Water / acetic acid mixture (Maxwell-Stephen)	-0.059	-0.0144	-0.0069	-0.013	0.0093
Water / Acetone Mixture (Fick Law)	-0.023	-0.042	-0.14	-0.21	0.415
Water / acetone mixture (Maxwell-Stephen)	-0.023	-0.01	-0.02	-0.038	0.091

4 - CONCLUSION

In this research, the design and simulation of pervaporation systems have been investigated. In CFD code simulation concerning mass transfer as well as motion transfer, a two-dimensional mathematical model has been used in this research. The process studied in this work involves the removal of water from a solution of acetone/water and acetic acid/water using a dense membrane. Evaporation is considered a separation method in which the separation is achieved by applying vacuum pressure on the infiltration side. Thus the vapor pressure gradient is the main driving force of the process. The Wilk-Chang method was used to estimate the diffusion mass transfer in the model and the liquid velocity was modeled using the Navier-Stokes equation. The finite element method was used to numerically solve the model equation and the results showed that increasing the feed rate reduces water removal due to reducing the residence time of the nutrient solution in the membrane module. In the feed section, the concentration changes near the membrane wall are high and in the areas far from the membrane, the concentration changes are low. In the membrane section, because the vacuum condition is assumed and only water passes through the membrane, as we move in the x-direction, the water concentration decreases and reaches zero at the membrane boundary.

In neural network simulation, the effect of operating conditions on the evaporation process is shown to increase with increasing temperature and water mass fraction in the flux feed. Dehydration of the feed was modeled using the evaporation process in the ANN process, which was shown to reflect the ANN error correctly. Input compounds include (10% water / 90% acetic acid and 10% water / 90% acetone). The error rates of these compounds at 50 °C are 0.9898, and 0.00332 respectively. Input compounds include (10% water / 90% acetic acid and 10% water / 90% acetone). The amount of error obtained from comparing experimental data and Fick model -0.0217 and -0.0442 and the amount of error obtained from comparing experimental data with Maxwell-Stephan model, respectively, -0.0144 and -0.01. In mathematical modeling, by comparing the laboratory data with the data obtained from the models, it is found that the Maxwell-Stephen model is consistent with the laboratory data and can predict the flux through the membrane with less error than the laboratory data.

REFERENCE

[1] Baker, R.W., Membrane technology and application, 2nd Edition, John Wiley, 2004.

[2] Wee, S.L., Tye, C.T., Bhatia, S. 2008. Membrane separation process-Pervaporation through zeolite membrane, Separation and Purification Technology, 63, 500–516.

[3] Nunes, S.P., Peinemann, K.V., Membrane Technology in the chemical industry, Wiley-VCH Verlag GmbH, 2001.

[4] Devos R., Verweij H.1998. High-Selectivity, High-Flux Silica Membranes for Gas Separation, Science, 279, 1710-1711.

[5] Motuzas, J., Heng, S., Ze Lau, P.P.S.2007. Ultra-rapid production of MFI membranes by coupling microwave-assisted synthesis with either ozone or calcination treatment, Microporous and Mesoporous Materials, 99, 197–205

[6] Moulik, S., Nazia, S., Vani, B., Sridhar, S. 2016.Pervaporation separation of acetic acid/water mixtures through sodium alginate/polyaniline polyion complex membrane, Sep. Purif. Technol. 170,30-39.

[7] Christopher J.C.W., Tsuji, K., Takewaki, T., Beck, L.W., Davis, M.E.2001. Tailoring molecular sieve properties during SDA

removal via solvent extraction, Microporous and Mesoporous Materials, 48, 57–64.

[8] Grose, R.W., Flanigen, E.M. Novel zeolite compositions and processes for preparing and using same, US Patent, 4257885, 1981.

[9] Prasad, N.S., Moulik, S., Bohra, S., Rani, K.Y., Sridhar, S.2016. Solvent resistant chitosan / poly (ether-blockamide) composite membranes for pervaporation ofn-methyl-2-pyrrolidone / water mixtures, Carbohyd. Polymers, 136(20) January, 170-1181

[10] Akhtar, F., Sjöberg, E., Korelskiy, D., Rayson, M., Hedlund, J., Bergström, L. 2015. Preparation of gradedsilicalite-1 substrates for all-zeolite membranes with excellent CO2/H2 separation performance, J.Membrane Sci. 493, 206-211.

[11] Bowen, T.C, Noble, R.D., Falconer, J.L 2004. Fundamentals and applications of pervaporation through zeolite membranes, Journal of membrane science, 245,1-33.

[12] Dyer, A., Introduction to Zeolite Molecular Sieves, John Wiley & Sons, New York,1988.

[13] Thakur, D.S., Thomas, M. G.1984. Catalyst Deactivation during Direct Coal Liquefacation, Indusial& Engineering Chemistry Product Research and Development, 23, 349-360.

[14] A.J. Toth, E. Haaz, T. Nagy, R. Tari, A.J. Tarjani, D. Fozer, A. Szanyi, K.-A. Koczka, L.Racz, G. Ugro, P. Mizsey, Evaluation of the accuracy of modelling the separation of highly non-ideal mixtures: extractive heterogeneous-azeotropic distillation, in: A. Espuña, M.Graells, L. Puigjaner (Eds.) Computer Aided Chemical Engineering, Elsevier, 2017, pp. 241-246.

[15] Schoeman, B. J., Sterte, J., Otterstedt, J. E.1994. Analysis of the crystal growth mechanism of TPA-silicalite-1, Zeolites, 14, 568-575.

[16] A.J. Toth, Liquid Waste Treatment with Physicochemical Tools for Environmental Protection, PhD Thesis, Budapest University of Technology and Economics, Budapest, 2015,pp. 197.

[17] Milton, W.M.1968. Molecular Sieves, Society of Chemical Industry, London, 1968.

[18] Dana, E.S., System of Mineralogy, John Wiley & Sons, New York, 1942.

[19] Nai, S., Liu X., Liu, W., Zhang, B.2015. Ethanol recoveryfrom its dilute aqueous solution using Fe-ZSM-5membranes: Effect of defect size and surface hydrophobicity, Micropor. Mesopor. Mat. 215, 46-50.

[20] VanBekkum H., Flanigen, E. M., Jansen J. C.1991. Introduction to Zeolite Science and Practice, Studies in Surface Science and Catalysis, 58. Amsterdam: Elsevier,1991.

[21] Xu, Y.M., Chung, T-S. 2017. High-performance UiO-66/polymide mixed matrix membranes for ethanol, isopropanol and n-butanol dehydration via pervaporation, J. Membrane Sci. 531, 16-26.

[22] Liao, Y-L., Hu, C-C., Lai, J-Y., Liu, Y-L. 2017. Cross linked polybenzoxazine based membrane exhibiting in-situ self-promoted separation performance for pervaporation dehydration on isopropanol aqueous solutions, J. Membrane Sci. 531, 10-15.

All © 2023 are reserved by International Journal of Advanced Science and Engineering. This Journal is licensed under a Creative Commons Attribution-Non Commercial-ShareAlike 3.0 Unported License.